

# Ultra High Energy Cosmic Rays from Compact Sources

Z. Fodor and S.D. Katz

*Institute for Theoretical Physics, Eötvös University,*

*Pázmány 1, H-1117 Budapest, Hungary*

(February 24, 2019)

The clustering of ultra high energy (above  $10^{20}$  eV) cosmic rays (UHECR) suggests that they might be emitted by compact sources. Statistical analysis of Dubovsky et al. (astro-ph/0001317) estimated the source density. We extend their analysis to give also the confidence intervals for the source density using a.) no assumptions on the relationship between clustered and unclustered events; b.) nontrivial distributions for the source intensities and energies; c.) the energy dependence of the propagation. We also determine the probability that a proton created at a distance  $r$  with energy  $E$  arrives at earth above a threshold  $E_c$ . The observed 14 UHECR events above  $10^{20}$  eV with one doublet gives for the source densities  $15.8_{-14.8}^{+334} \cdot 10^{-3} \text{ Mpc}^{-3}$  (on the 68% confidence level). We present detailed results for future experiments with larger UHECRs statistics.

## I. INTRODUCTION

The interaction of protons with photons of the cosmic microwave background predicts a sharp drop in the cosmic ray flux above the GZK cutoff around  $5 \cdot 10^{19}$  eV [1]. The available data shows no such drop. About 20 events above  $10^{20}$  eV were observed by a number of experiments such as AGASA [2], Fly's Eye [3], Haverah Park [4], Yakutsk [5] and HiRes [6]. Since above the GZK energy the attenuation length of particles is a few tens of megaparsecs [7] if an ultra high energy cosmic ray (UHECR) is observed on earth it must be produced in our vicinity (except for UHECR scenarios based on weakly interacting particles, e.g. neutrinos).

Usually it is assumed that at these high energies the galactic and extragalactic magnetic fields do not affect the orbit of the cosmic rays, thus they should point back to their origin within a few degrees. In contrast to the low energy cosmic rays one can use UHECRs for point-source search astronomy (for an extragalactic magnetic field of  $\mu\text{G}$  rather than the usually assumed  $\text{nG}$  there is no directional correlation with the source [8]). Though there are some peculiar clustered events, which we discuss in detail, the overall distribution of UHECR on the sky is practically isotropic. This observation is rather surprising since in principle only a few astrophysical sites (e.g. active galactic nuclei [9] or the extended lobes of radio galaxies [10]) are capable of accelerating such particles, nevertheless none [11] of the UHECR events came from these directions. Hence it is generally believed [12] that there is no conventional astrophysical explanation for the observed UHECR spectrum.

There are several ways to look for the source inhomogeneity from the energy spectrum and spatial directions of UHECRs. One possibility is to assume that the source density of UHECRs is proportional to the galaxy densities [13]. Another approach is to analyze the clustering

properties of the unknown sources by some correlation length [14].

Clearly, the arrival directions of the UHECRs measured by experiments show some peculiar clustering: some events are grouped within  $\sim 3^\circ$ , the typical angular resolution of an experiment. Above  $4 \cdot 10^{19}$  eV 92 cosmic ray events were detected, including 7 doublets and 2 triplets. Above  $10^{20}$  eV one doublet out of 14 events were found [15]. The chance probability of such a clustering from uniform distribution is rather small [15,16].

The clustered features of the events initiated an interesting statistical analysis assuming compact UHECR sources [17]. The authors found a large number,  $\sim 400$  for the number of sources \* inside a GZK sphere of 25 Mpc. They assumed that

- a. the number of clustered events is much smaller than the total number of events (this is a reliable assumption at present statistics; however, for any number of sources the increase of statistics, which will happen in the near future, results in more clustered events than unclustered),
- b. all sources have the same intensity which gives a delta function for their distribution (this unphysical choice represents an important limit, it gives the smallest source density for a given number of clustered and unclustered events)

---

\*approximately 400 sources within the GZK sphere results in one doublet for 14 events. The order of magnitude of this result is in some sense similar to that of a "high-school" exercise: what is the minimal size of a class for which the probability of having clustered birthdays –at least two pupils with the same birthdays– is larger than 50%. In this case the number of "sources" is the number of possible birthdays  $\sim 400$ . In order to get the answer one should solve  $365!/[365^k(365-k)!] < 0.5$ , which gives  $k=23$ .

c. The GZK effect makes distant sources fainter; however, this feature depends on the injected energy spectrum and the attenuation lengths and elasticities of the propagating particles. In [17] an exponential decay was used with an energy independent decay length of 25Mpc.

In our approach none of these assumptions are used. In addition we include spherical astronomy corrections and in particular give the upper and lower bounds for the source density at a given confidence level. As we show the most probable value for the source density is really large; however, the statistical significance of this result is rather weak. At present the small number of UHECR events allows a 95% confidence interval for the source density which spreads over four orders of magnitude. Since future experiments, particularly Pierre Auger [18,19], will have a much higher statistical significance on clustering (the expected number of events of  $10^{20}$  eV and above is 60 per year [20]), we present our results on the density of sources also for larger number of UHECRs above  $10^{20}$  eV.

In order to avoid the assumptions of [17] a combined analytical and Monte-Carlo technique will be presented adopting the conventional picture of protons as the ultra high energy cosmic rays. Our analytical approach of Section 2 gives the event clustering probabilities for any space, intensity and energy distribution of the sources by using a single additional function  $P(r, E; E_c)$ , the probability that a proton created at a distance  $r$  with energy  $E$  arrives at earth above the threshold energy  $E_c$  [14]. With our Monte-Carlo technique of Section 3 we determine the probability function  $P(r, E; E_c)$  for a wide range of parameters. Our results for the present and future UHECR statistics are presented in Section 4. We summarize in Section 5.

## II. ANALYTICAL APPROACH

The key quantity for finding the distribution functions for the source density is the probability of detecting  $k$  events from one randomly placed source. The number of UHECRs emitted by a source during a period  $T$  follows the Poisson distribution. The probability that the source emits  $k$  UHECRs is:

$$p_k = \frac{e^{-\lambda T}}{k!} (\lambda T)^k, \quad (1)$$

where  $\lambda$  is the intensity of the source. However, not all emitted UHECRs will be detected. They might loose their energy during propagation or can simply go to the wrong direction.

For UHECRs the energy loss is dominated by the pion production in interaction with the cosmic microwave background radiation. In ref. [14] the probability function  $P(r, E, E_c)$  was presented for three specific threshold energies. This function gives the probability that a proton created at a given distance from earth (r) with some

energy (E) is detected at earth above some energy threshold ( $E_c$ ). The resulting probability distribution can be approximated over the energy range of interest by a function of the form

$$P(r, E, E_c) = \exp[-a(E_c)r^2 \exp(b(E_c)/E)] \quad (2)$$

The appropriate values of  $a$  and  $b$  for  $E_c/(10^{20}\text{eV}) = 1, 3, 6$  are, respectively  $a/(10^{-4}\text{Mpc}^{-2}) = 1.4, 9.2$  and  $11, b/(10^{20}\text{eV}) = 2.4, 12$  and  $28$ .

For the sources we use the second equatorial coordinate system:  $\mathbf{x}$  is the position vector of the source characterized by  $(r, \theta, \phi)$  with  $\theta$  and  $\phi$  being the polar angle and right ascension, respectively. The features of the Poisson distribution enforce us to take into account the fact that the sky is not isotropically observed. There is a circumpolar cone, in which the sources can always be seen, with half opening angle  $\pi/2 - \alpha$  ( $\alpha$  is the polar angle of the detector, for the experiments we study  $\alpha \approx 40^\circ - 50^\circ$ ). There is also an invisible region with the same opening angle. Between them there is a region for which the time fraction of visibility,  $\gamma(\theta, \alpha)$  is a function of the polar angle of the source. It is straightforward to determine  $\gamma(\theta, \alpha)$  for any  $\theta$  and  $\alpha$ :

$$\gamma(\theta, \alpha) = \begin{cases} 1 & \text{if } 0 < \theta \leq \pi/2 - \alpha \\ 1 - \arccos(\cot \alpha \cot \theta)/\pi & \text{if } \pi/2 - \alpha < \theta \leq \pi/2 + \alpha \\ 0 & \text{if } \pi/2 + \alpha < \theta \leq \pi \end{cases} \quad (3)$$

To determine the probability that a particle arriving from random direction at a random time is detected we have to multiply  $\gamma(\theta, \alpha)$  by the cosine of the zenith angle. ([17] neglected these effects, which mean more than a factor of two for the prediction of the source density.) In the following we will use the time average of this function,  $\eta(\theta, \alpha)$  and do not indicate the  $\alpha$  dependence.

The probability of detecting  $k$  events from a source at distance  $r$  with energy  $E$  can be obtained by including  $P(r, E, E_c)A\eta(\theta)/(4\pi r^2)$  in eqn. (1):

$$p_k(\mathbf{x}, E, j) = \frac{\exp[-P(r, E, E_c)\eta(\theta)j/r^2]}{k!} \times [P(r, E, E_c)\eta(\theta)j/r^2]^k, \quad (4)$$

where we introduced  $j = \lambda T A / (4\pi)$  and  $A/(4\pi r^2)$  is the probability that an emitted UHECR points to a detector of area  $A$ . For simplicity we call  $j$  "source intensity" in the rest of the paper. We denote the space, energy and intensity distributions of the sources by  $\rho(\mathbf{x})$ ,  $c(E)$  and  $h(j)$ , respectively. The probability of detecting  $k$  events above the threshold  $E_c$  from a single source randomly positioned within a sphere of radius  $R$  is

$$P_k = \int_{S_R} dV \rho(\mathbf{x}) \int_{E_c}^{\infty} dE c(E) \int_0^{\infty} dj h(j) \times \frac{\exp[-P(r, E, E_c)\eta(\theta)j/r^2]}{k!} [P(r, E, E_c)\eta(\theta)j/r^2]^k. \quad (5)$$

Denote the total number of sources within the sphere of sufficiently large radius (e.g. several times the GZK radius) by  $N$  and the number of sources that gave  $k$  detected events by  $N_k$ . Clearly,  $N = \sum_0^\infty N_i$  and the total number of detected events is  $N_e = \sum_0^\infty i N_i$ . The probability that for  $N$  sources the number of different detected multiplets are  $N_k$  is:

$$P(N, \{N_k\}) = N! \prod_{k=0}^{\infty} \frac{1}{N_k!} P_k^{N_k}. \quad (6)$$

The value of  $P(N, \{N_k\})$  is the most important quantity in our analysis of UHECR clustering. For a given set of unclustered and clustered events ( $N_1$  and  $N_2, N_3, \dots$ ) inverting the  $P(N, \{N_k\})$  distribution function gives the most probable value for the number of sources and also the confidence interval for it. If we want to determine the density of sources we can take the limit  $R \rightarrow \infty, N \rightarrow \infty$ , while the density of sources  $S = N/(\frac{4}{3}R^3\pi)$  is constant.

In order to illustrate the dominant length scale it is instructive to study the integrand  $f_k(r)$  of the distance integration in eqn. (5)

$$P_k = \int_0^R dr f_k(r),$$

$$f_k(r) = r^2 \int d\Omega \rho(\mathbf{x}) \int_{E_c}^{\infty} dE c(E) \int_0^{\infty} dj h(j) \times$$

$$\exp \left[ -P(r, E, E_c) \eta(\theta) j / r^2 \right] [P(r, E, E_c) \eta(\theta) j / r^2]^k. \quad (7)$$

Fig. 1 shows that  $f_1(r)$ , which leads to singlet events, is dominated by the distance scale of 10-15 Mpc, whereas  $f_2(r)$ , which gives doublet events, is dominated by the distance scale of 3-5 Mpc. These typical distances partly justify our assumption of neglecting magnetic fields. The deflection of singlet events due to magnetic field does not change the number of multiplets, thus our conclusions. The typical distance for higher multiplets is quite small, therefore deflection can be practically neglected. Clearly, the fact that multiplets are coming from our “close” neighbourhood does not mean that the experiments reflect just the densities of these distances. The overwhelming number of events are singlets and they come from much larger distances. Note, that these  $f_1(r)$  and  $f_2(r)$  functions are obtained with our optimal  $j_*$  intensity (cf. Fig. 5 and explanation there and in the corresponding text). Using the largest possible  $j_*$  intensity allowed by the 95% confidence region the dominant distance scales for  $f_1(r)$  and  $f_2(r)$  functions turn out to be 30 Mpc and 20 Mpc, respectively.

Note, that  $P_k$  and then  $P(N, \{N_k\})$  are easily determined by a well behaving four-dimensional numerical integration (the *phi* integral can be factorized) for any  $c(E)$ ,  $h(j)$  and  $\rho(r)$  distribution functions. In order to illustrate the uncertainties and sensitivities of the results

we used a few different choices for these distribution functions.

For  $c(E)$  we studied three possibilities. The most straightforward choice is the extrapolation of the ‘conventional high energy component’  $\propto E^{-2}$ . Another possibility is to use a stronger fall-off of the spectrum at energies just below the GZK cutoff, e.g.  $\propto E^{-3}$ . These choices span the range usually considered in the literature and we will study both of them. The third possibility is to assume that UHECRs are decay products of metastable superheavy particles <sup>†</sup> [24,25]. According to [25] these superheavy particles decay into quarks and gluons which initiate multi-hadron cascades through gluon bremsstrahlung. These finally hadronize to yield jets. The energy spectrum in this case can be estimated by the function obtained from the HERWIG QCD generator:

$$c(x) = c_1 \frac{\exp[c_2 \sqrt{\ln(1/x)}](1-x)^2}{x \sqrt{\ln(1/x)}}, \quad (8)$$

where  $x = E/m_X$  the ratio of the energy and the mass of the decaying particle. The best fit [25] to the observed UHECR spectrum gives  $m_X \approx 10^{12}$  GeV for the mass of the decaying particle. This corresponds to  $c_1 \approx 0.0086$  and  $c_2 \approx 2.77$ . We will use these  $c_1$  and  $c_2$  values for our third choice of energy distribution,  $c(E)$ .

In ref. [17] the authors have shown that for a fixed set of multiplets the minimal density of sources can be obtained by assuming a delta-function distribution for  $h(j)$ . We studied both this limiting case ( $h(j) = \delta(j - j_*)$ ) and a more realistic one with a distribution function spreading over an order of magnitude:

$$h(j) = h \cdot \exp[\log_{10}(j/j_*)^2/2]. \quad (9)$$

The space distribution of sources can be given based on some particular survey of the distribution of nearby galaxies [13] or on a correlation length  $r_0$  characterizing the clustering features of sources [14]. For simplicity the present analysis deals with a homogeneous distribution of sources randomly scattered in the universe.

Fig. 2 shows the resulting  $P_k(j_*)$  probability functions for the different choices of  $c(E)$  and  $h(j)$ . The overall shapes of them are rather similar; nevertheless, relatively small differences lead to quite different predictions for the UHECR source density. The “shoulders” of the curves with Dirac-delta intensity distributions got smoother for the distribution spreading over an order of magnitude. The  $j_*$  scales for the different intensity distributions are different. The reason for this is that for the spread distribution the dominant  $j$  values are not around the center,

---

<sup>†</sup>The possibility of superheavy relic particles had been proposed before the observation of UHECR beyond the GZK cutoff [23].

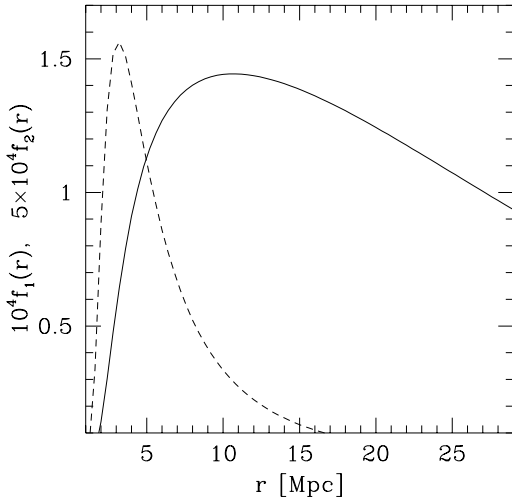


FIG. 1. The distributions  $f_1(r)$  –solid line– and  $f_2(r)$  –dashed line– of eqn. (7). The singlet and doublet events are dominated by distance scale of 10-15 Mpc and 3-5 Mpc, respectively.

$j_*$  but they are larger by about three orders of magnitude. The scales on the figures are chosen to cover the 98% confidence regions (see section IV for details).

Note, that – assuming that UHECRs point back to their sources – our clustering technique discussed above applies to practically any models of UHECR (e.g. neutrinos). One only needs a change in the  $P(r, E, E_c)$  probability distribution function (e.g. neutrinos penetrate the microwave background uninhibited) and use the  $h(j)$  and  $c(E)$  distribution function of the specific model.

### III. MONTE-CARLO STUDY OF THE PROPAGATION

Our Monte-Carlo model of UHECR studies the propagation of UHECR. The analysis of [21] showed that both AGASA and Fly's Eye data demonstrated a change of composition, a shift from heavy –iron– at  $10^{17}$  eV to light –proton– at  $10^{19}$  eV. Thus, the chemical composition of UHECRs is most likely to be dominated by protons. In our analysis we use exclusively protons as UHECR particles. (for suggestions that air showers above the GZK cutoff are induced by neutrinos see [22].)

Using the pion production as the dominant effect of energy loss for protons at energies  $> 10^{19}$  eV ref. [14] calculated  $P(r, E, E_c)$ , the probability that a proton created at a given distance ( $r$ ) with some energy ( $E$ ) is detected at earth above some energy threshold ( $E_c$ ). For three threshold energies the authors of [14] gave an approximate formula, which we used in the previous section.

In our Monte-Carlo approach we determined the propagation of UHECR on an event by event basis. Since

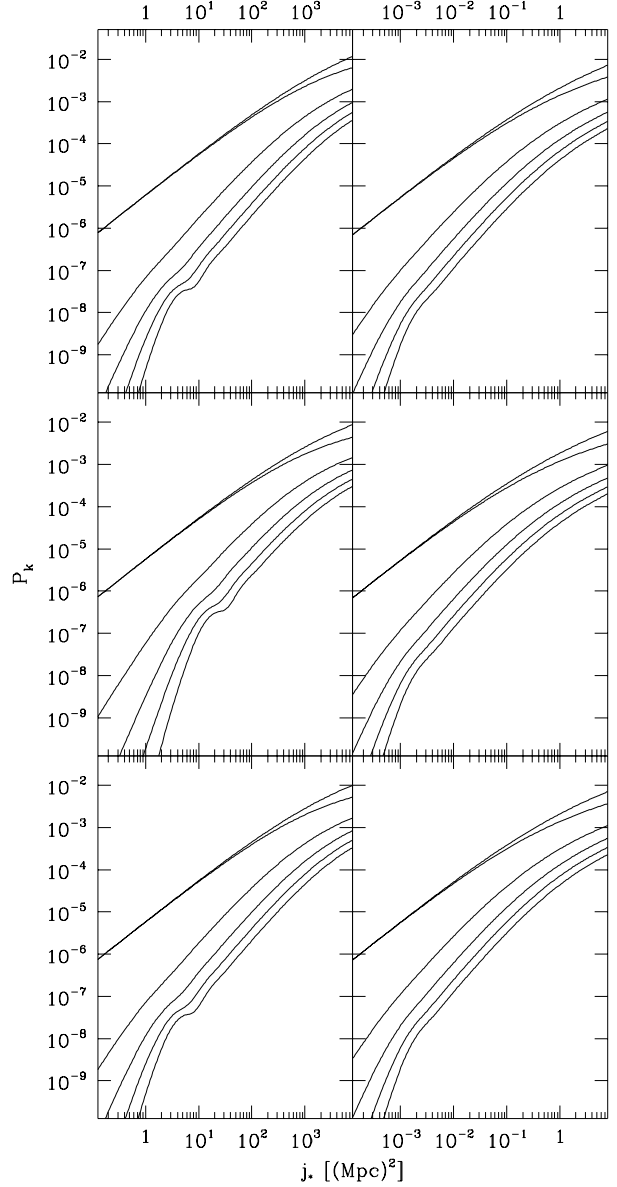


FIG. 2. The individual  $P_k(j_*)$  functions for the different  $c(E)$  and  $h(j)$  choices. The column on the left corresponds to the Dirac-delta distribution  $h(j) = \delta(j - j_*)$ , whereas the column on the right shows the results for a distribution spreading over an order of magnitude  $h(j) = h \cdot \exp[-\log_{10}(j/j_*)^2/2]$ . The first, second and third rows correspond to the  $c(E)$  functions proportional to  $E^{-2}$ ,  $E^{-3}$  and the superheavy decay mode, respectively (see text). On each panel the individual lines from top to bottom are: 1 –  $P_0$ ,  $P_1$ ,  $P_2$ ,  $P_3$ ,  $P_4$  and  $P_5$ .

the inelasticity of Bethe-Heitler pair production is rather small ( $\approx 10^{-3}$ ) we used a continuous energy loss approximation for this process. The inelasticity of pion-photoproduction is much higher ( $\approx 0.2 - 0.5$ ) in the energy range of interest, thus there are only a few tens of such interactions during the propagation. Due to the Poisson statistics of the number of interactions and the spread of the inelasticity, we will see a spread in the energy spectrum even if the injected spectrum is mono-energetic.

In the simulation protons are propagated in small steps ( $10\text{kpc}$ ), and after each step the energy losses due to pair production, pion production and the adiabatic expansion are calculated. During the simulation we keep track of the current energy of the proton and its total displacement. This one avoids performing new simulations for different initial energies and distances. The propagation is completed when the energy of the proton goes below a given cutoff. For the proton interaction lengths and inelasticities we used the values of [26,27]. The deflection due to magnetic field is not taken into account, because it is small for our typical distances illustrated in Fig. 1. This fact justifies our assumption that UHECRs point back to their sources (for a recent Monte-Carlo analysis on deflection see e.g. [28]).

Since it is rather practical to use the  $P(r, E, E_c)$  probability distribution function we extended the results of [14] by using our Monte-Carlo technique for UHECR propagation. In order to cover a much broader energy range than the parametrization of (2) we used the following type of function

$$P(r, E, E_c) = \exp [-a \cdot (r/1 \text{ Mpc})^b]. \quad (10)$$

Fig. 3 demonstrates the reliability of this parametrization. The direct Monte-Carlo points and the fitted function (eqn. (10) with  $a = 0.0019$  and  $b = 1.695$ ) are plotted for  $E_c = 10^{20}\text{eV}$  and  $E = 2 \cdot 10^{20}\text{eV}$ . Fig. 4 shows the the functions  $a(E/E_c)$  and  $b(E/E_c)$  for a range of three orders of magnitude and for five different threshold energies. Just using the functions of  $a(E/E_c)$  and  $b(E/E_c)$ , thus a parametrization of  $P(r, E, E_c)$  one can obtain the observed energy spectrum for any injection spectrum without additional Monte-Carlo simulation.

#### IV. RESULTS

In order to determine the confidence intervals for the source densities we used the frequentist method [29]. We wish to set limits on  $S$ , the source density. Using our Monte-Carlo based  $P(r, E, E_c)$  functions and our analytical technique we determined  $p(N_1, N_2, N_3, \dots; S; j_*)$ , which gives the probability of observing  $N_1$  singlet,  $N_2$  doublet,  $N_3$  triplet etc. events if the true value of the density is  $S$  and the central value of intensity is  $j_*$ . The probability distribution is not symmetric and far from being Gaussian. For a given set of  $\{N_i, i = 1, 2, \dots\}$  the

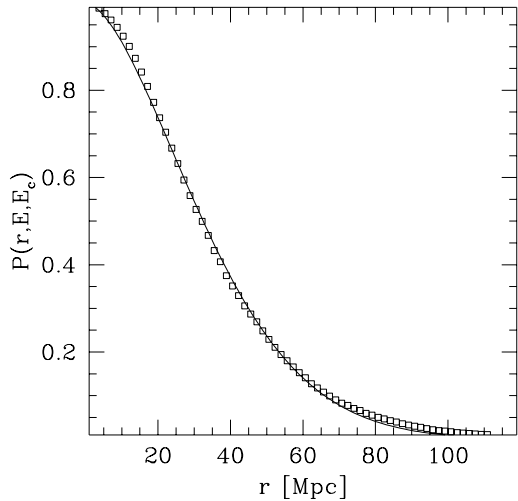


FIG. 3. The direct Monte-Carlo points and the fitted function  $P(r, E, E_c) = \exp [-a \cdot (r/1\text{Mpc})^b]$  for  $E_c = 10^{20}\text{ eV}$  and  $E = 2 \cdot 10^{20}\text{ eV}$ . The fitted curve corresponds to  $a = 0.0019$  and  $b = 1.695$ .

above probability distribution as a function of  $S$  and  $j_*$  determines the 68% and 95% confidence level regions in the  $S - j_*$  plane. Fig. 5 shows these regions for our “favorite” choice of model ( $c(E) \propto E^{-3}$  and the luminosity distribution spreading over an order of magnitude) and for the present statistics (one doublet out of 14 UHECR events). The regions are deformed, thin ellipse-like objects in the  $\log(j_*)$  versus  $\log(S)$  plane. Since the source intensity is a completely unknown and independent physical quantity the source density can be anything between the bottom and the top of the confidence level regions. For this model our final answer for the density is  $15.8_{-14.8(15.6)}^{+334(3360)} 10^{-3} \text{ Mpc}^{-3}$ , where the first error indicate the 68%, the second one in the parenthesis the 95% confidence levels, respectively. The choice of [17] – Dirac-delta like intensity distribution– and, for instance, conventional  $E^{-2}$  energy distribution gives smaller value:  $2.77_{-2.53(2.70)}^{+96.1(916)} 10^{-3} \text{ Mpc}^{-3}$ . For other choices of  $c(E)$  and  $h(j)$  see Table I. Our results are in agreement with the result of [17] within the error bars. Nevertheless, there is a very important message. The confidence level intervals are so large, that on the 95% confidence level two orders of magnitude smaller densities than suggested as a lower bound by [17] are also possible.

As it can be seen there is a strong correlation between the source intensity and the source density. Physically it is easy to understand the picture. For a smaller source density the intensities should be larger to give the same number of events. However it is not possible to produce the same multiplicity structure with arbitrary intensities. Very small intensities can not give multiplets at all, very large intensities tend to give more than one doublet.

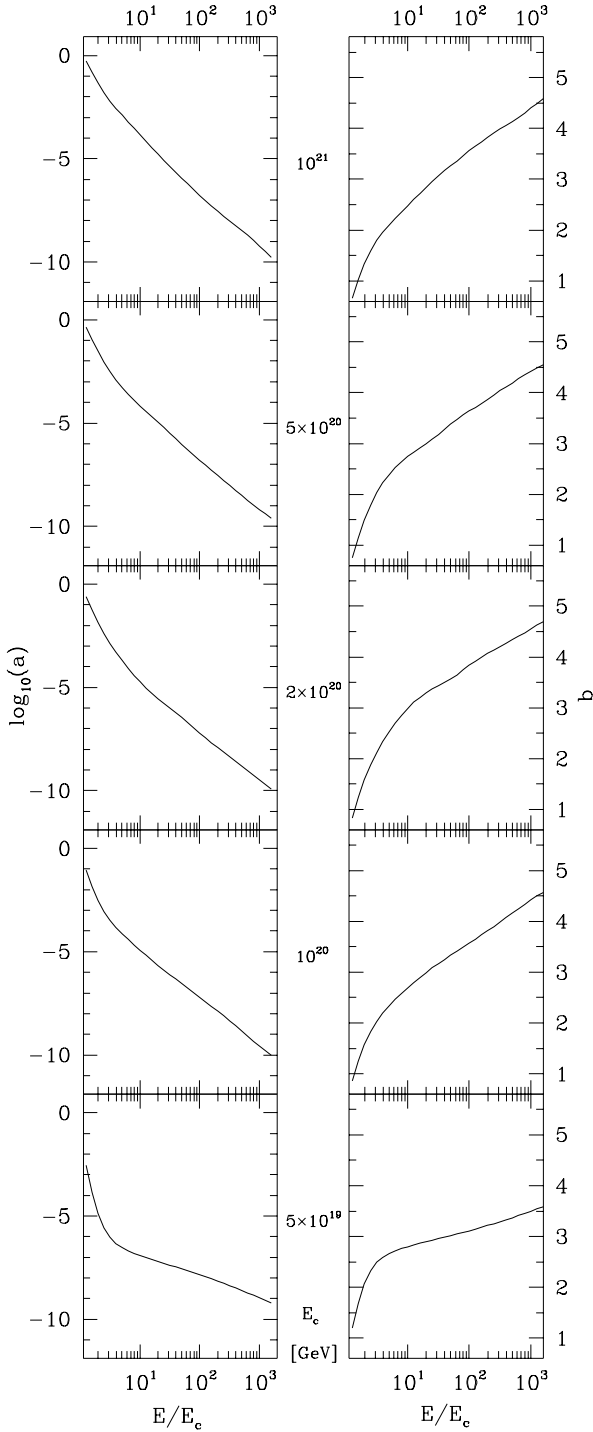


FIG. 4. The functions  $a(E/E_c)$  –left panel– and  $b(E/E_c)$  –right panel– for the probability distribution function  $P(r, E, E_c)$  using the parametrization  $\exp[-a \cdot (r/1 \text{ Mpc})^b]$  for five different threshold energies ( $5 \cdot 10^{19} \text{ eV}$ ,  $10^{20} \text{ eV}$ ,  $2 \cdot 10^{20} \text{ eV}$ ,  $5 \cdot 10^{20} \text{ eV}$  and  $10^{21} \text{ eV}$ ).

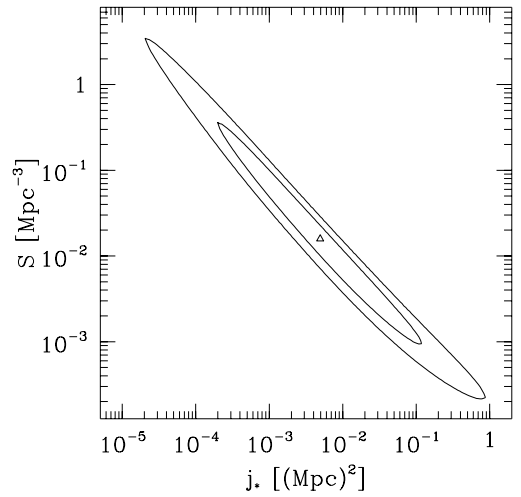


FIG. 5. The  $1\sigma$  (68%) and  $2\sigma$  (95%) confidence level regions for the normalized source intensity and source density (14 UHECR with one doublet). The most probable value is represented by the triangle. The upper and lower boundaries of these regions give for the source density  $15.8^{+334(3360)}_{-14.8(15.6)} 10^{-3} \text{ Mpc}^{-3}$  on the 68% (95%) confidence level.

The same technique can be applied for any hypothetical experimental result. For fixed  $\{N_k\}$  the above probability function determines the 68% confidence regions in  $S$  and  $j_*$ . Using these regions one can tell the 68% confidence interval for  $S$ . The most probable values of the source densities for fixed number of multiplets are plotted on Fig. 6 with the lower and upper bounds. The total number of events is shown on the horizontal axis, whereas the number of multiplets label the lines. Here again, our “favorite” choice of distribution functions were used:  $c(E) \propto E^{-3}$  and  $h(j)$  of eqn. (9).

It is of particular interest to analyze in detail the present experimental situation having one doublet out of 14 events. Since there are some new unpublished events, too, we study the a hypothetical case of one or two doublets out of 24 events. The 68% and 95% confidence level results are summarized in Table I for our three energy and two intensity distributions. It can be seen that Dirac-delta type intensity distribution really gives smaller source densities than broad intensity distribution, as it was proven by [17]. Less pronounced is the effect on the energy distribution of the emitted UHECRs. The difference between the individual results –thus for  $c(E) \propto E^{-2}$ ,  $E^{-3}$  or given by the decay of a superheavy particle– and some “central value” is always smaller than 50%. The confidence intervals are typically very large, on the 95% level they span 4 orders of magnitude. An interesting feature of the results is that “doubling” the present statistics with the same clustering features (in the case studied by the table this means one new doublet out of 10 new events) reduces the confidence level intervals by an

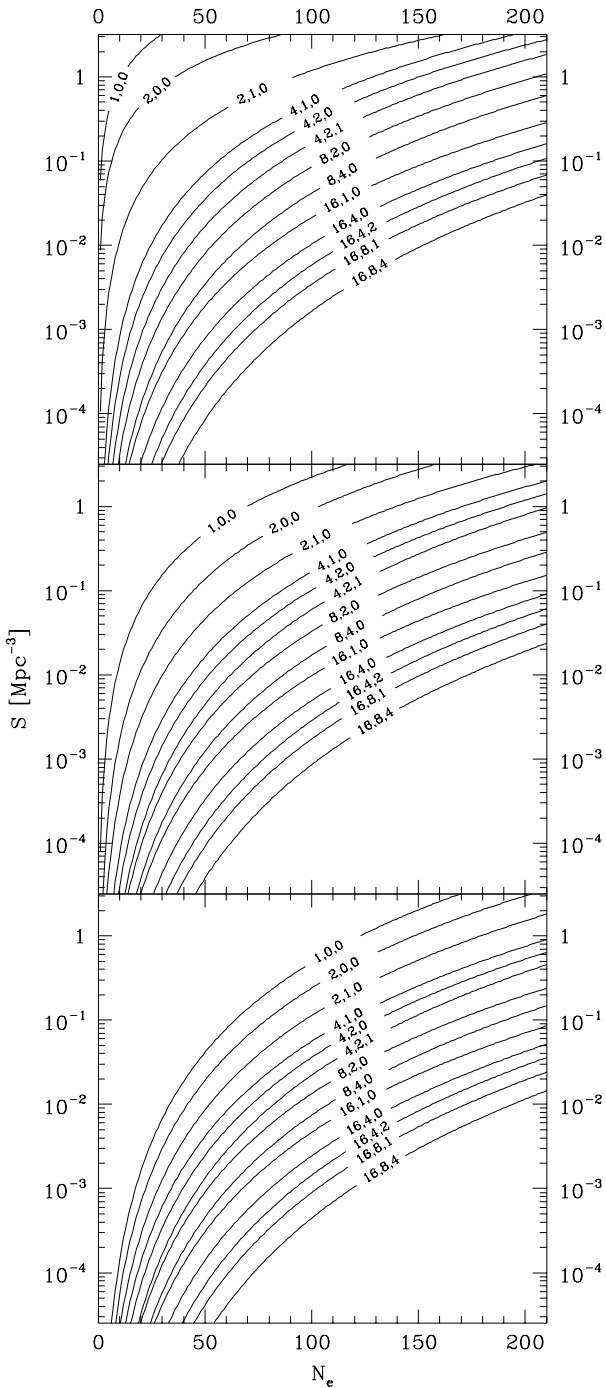


FIG. 6. The most probable values for the density of sources as a function of the total number of events (middle panel). The number of multiplets are indicated on the individual lines in the form:  $N_2, N_3, N_4$ , where  $N_2, N_3$  and  $N_4$  represent the appropriate values for doublets, triplets and quartets. The upper and lower panels correspond to the 84 percentile and 16 percentile lines (upper and lower bounds of the 68% confidence intervals), respectively.

order of magnitude. The reduction is far less significant if we add singlet events only. Inspection of Fig. 6 leads to the conclusion that experiments in the near future with approximately 200 UHECR events can tell at least the order of magnitude of the source density.

<b>14 events 1 doublet</b>		
$c(E)$	$h(j)$	
$\propto E^{-2}$	$\propto \delta$	$2.77^{+96.1(916)}_{-2.53(2.70)}$
$\propto E^{-2}$	$\propto \text{spread}$	$10.9^{+256(2840)}_{-10.2(10.7)}$
$\propto E^{-3}$	$\propto \delta$	$5.37^{+80.2(624)}_{-4.98(5.25)}$
$\propto E^{-3}$	$\propto \text{spread}$	$15.8^{+334(3360)}_{-14.8(15.6)}$
$\propto \text{decay}$	$\propto \delta$	$3.61^{+116(1060)}_{-3.30(3.51)}$
$\propto \text{decay}$	$\propto \text{spread}$	$11.9^{+268(2860)}_{-11.2(11.7)}$
<b>24 events 1 doublet</b>		
$c(E)$	$h(j)$	
$\propto E^{-2}$	$\propto \delta$	$17.4^{+298(2790)}_{-16.0(17.0)}$
$\propto E^{-2}$	$\propto \text{spread}$	$57.8^{+683(6170)}_{-52.9(56.6)}$
$\propto E^{-3}$	$\propto \delta$	$25.0^{+211(1690)}_{-22.6(24.3)}$
$\propto E^{-3}$	$\propto \text{spread}$	$77.7^{+837(7240)}_{-70.9(76.0)}$
$\propto \text{decay}$	$\propto \delta$	$20.4^{+358(3190)}_{-18.6(19.9)}$
$\propto \text{decay}$	$\propto \text{spread}$	$62.9^{+743(6220)}_{-57.8(61.5)}$
<b>24 events 2 doublets</b>		
$c(E)$	$h(j)$	
$\propto E^{-2}$	$\propto \delta$	$3.19^{+26.4(253)}_{-2.68(2.99)}$
$\propto E^{-2}$	$\propto \text{spread}$	$11.6^{+120(615)}_{-10.0(11.0)}$
$\propto E^{-3}$	$\propto \delta$	$6.42^{+46.2(193)}_{-5.46(6.07)}$
$\propto E^{-3}$	$\propto \text{spread}$	$16.9^{+157(741)}_{-14.4(16.1)}$
$\propto \text{decay}$	$\propto \delta$	$4.18^{+34.5(296)}_{-3.51(3.92)}$
$\propto \text{decay}$	$\propto \text{spread}$	$13.1^{+126(628)}_{-11.3(12.5)}$

TABLE I. The most probable values for the source densities and their error bars given by the 68% and 95% confidence level regions (the latter in parenthesis). The numbers are in units of  $10^{-3} \text{ Mpc}^{-3}$ . The three possible energy spectrums are given by a distribution proportional to  $E^{-2}$ ,  $E^{-3}$ , or by the decay of a  $10^{12} \text{ GeV}$  particle (denoted by “decay”). The luminosity distribution can be proportional to a Dirac-delta or to a function spreading over an order of magnitude (denoted by “spread”). Results are listed for the observed 1 doublet out of 14 events and for two hypothetical cases (1 doublet out of 24 events and 2 doublets out of 24 events).

## V. SUMMARY

We presented a technique in order to statistically analyze the clustering features of UHECR. The technique can be applied for any model of UHECR assuming small deflection. The key role of the analysis is played by the  $P_k$  functions defined by eqn. (5), which is the probability of detecting  $k$  events above the threshold from a single

source. Using a combinatorial expression of eqn. (6) the probability distribution for any set of multiplets can be given as a function of the source density.

We discussed several types of energy and intensity distributions for the sources and gave the most probable source densities with their confidence intervals for present and future experiments.

The probability  $P(r, E, E_c)$  that a proton created at a distance  $r$  with energy  $E$  arrives above the threshold  $E_c$  [14] is determined and parametrized for a wide range of threshold energies. This result can be used to obtain the observed energy spectrum of the UHECR for arbitrary injection spectrum.

In ref. [17] the authors analyzed the statistical features of clustering of UHECR, which provided constraints on astrophysical models of UHECR when the number of clusters is small, by giving a bound from below. In our paper we have shown that there is some constraint, but it is far from being tight. At present statistics the 95% confidence level regions usually span 4 orders of magnitude. Two orders of magnitude smaller numbers than the prediction of [17] (their eqn. (13) suggests for the density of sources  $\sim 6 \cdot 10^{-3} \text{ Mpc}^{-3}$ ) can also be obtained. Adding 10 new events with an additional doublet the confidence interval can be reduced to 3 orders of magnitude and the increase of the UHECR events to 200 can tell at least the order of magnitude of the source density.

## VI. ACKNOWLEDGEMENTS

We thank K. Petrovay for clarifying some issues in spherical astronomy. This work was partially supported by Hungarian Science Foundation grants No. OTKA-T29803/T22929-FKP-0128/1997.

---

- [1] K. Greisen, Phys. Rev. Lett. 16 (1966) 748; G.T. Zatsepin and V.A. Kuzmin, Pisma Zh. Exp. Teor. Fiz. 4 (1966) 114.
- [2] M. Takeda et al., Phys. Rev. Lett. 81 (1998) 1163; astro-ph/9902239; www-akeno.icrr.u-tokyo.ac.jp/AGASA/results.html#100EeV
- [3] D.J. Bird et al., Phys. Rev. Lett. 71 (1993) 3401; Astrophys J. 424 (1994) 491; ibid 441 (1995) 144.
- [4] M.A. Lawrence, R.J.O. Reid and A.A. Watson, J. Phys. G 17 (1991) 773.
- [5] N.N. Efimov et al. in Proc. Astrophysical Aspects of the Most Energetic Cosmic Rays, p. 20, eds. M. Nagano and F. Takahara, World Sci., Singapore, 1991.
- [6] D. Kieda et al., Proc. of the 26th ICRC, Salt Lake, 1999; www.physics.utah.edu/Resrch.html
- [7] S. Yoshida, M. Teshima, Prog. Theor. Phys. 89 (1993) 833;

- F.A. Aharonian, J.W. Cronin, Phys. Rev. D50 (1994) 1892;
- R.J. Protheroe, P. Johnson, Astropart. Phys. 4 (1996) 253.
- [8] G.R. Farrar and T. Piran, Phys. Rev. Lett. 84 (2000) 3527; A. Dar, astro-ph/0006013.
- [9] K. Mannheim, Astropart. Phys. 3 (1995) 295.
- [10] J.P. Rachen, P.L. Biermann, Astron. Astrophys. 272 (1993) 161.
- [11] J.W. Elbert, P. Sommers, Astrophys. J. 441 (1995) 151.
- [12] R.D. Blandford, Phys. Scr. T85 (2000) 191Phys. Scr. T85 (2000) 191.
- [13] E. Waxman, K.B. Fisher and T. Piran, Astrophys. J. 483 (1997) 1; M. Giller, J. Wdowczyk and A. Wolfendale, J. Phys. G6 (1980) 1561; C.T. Hill and D.N. Schramm, Phys. Rev. D31 (1985) 564.
- [14] J.N. Bahcall and E. Waxman, hep-ph/9912326.
- [15] Y. Uchihori et al., Astropart. Phys. 13 (2000) 151-160.
- [16] N. Hayashida et al., Phys. Rev. Lett. 77 (1996) 1000.
- [17] S.L. Dubovsky, P.G. Tinyakov and I.I. Tkachev, astro-ph/0001317.
- [18] M. Boratav, Nucl. Phys. Proc. 48 (1996) 488.
- [19] C.K. Guerard, Nucl. Phys. Proc. 75A (1999) 380.
- [20] X. Bertou, M. Boratav, A. Letessier-Selvon, astro-ph/0001516.
- [21] B.R. Dawson, R. Meyhandan and K.M. Simpson, Astropart. Phys. 9 (1998) 331.
- [22] G. Domokos, S. Nussinov, Phys. Lett. B187 (1987) 372; T.J. Weiler, Astropart. Phys. 11 (1999) 303, Astropart. Phys. 12 (2000) 379 (Erratum); G. Domokos, S. Kovesi-Domokos and P.T. Mikulski, hep-ph/0006328.
- [23] J. Ellis, J.L. Lopez, D.V. Nanopoulos, Phys. Lett. B247 (1990) 257; J. Ellis et al., Nucl. Phys. B373 (1992) 399; P. Gondolo, G.B. Gelmini, S. Sarkar, Nucl. Phys. B392 (1993) 111.
- [24] V. Berezinsky, M. Kachelrieß and A. Vilenkin, Phys. Rev. Lett. 79 (1997) 4302; V.A. Kuzmin, V.A. Rubakov, Phys. Atom. Nucl. 61 (1998) 1028.
- [25] M. Birkel and S. Sarkar, Astropart. Phys. 9 (1998) 297; S. Sarkar, hep-ph/0005256.
- [26] P. Bhattacharjee and G. Sigl, Phys. Rep. 327 (2000) 109.
- [27] A. Achterberg et al., astro-ph/9907060.
- [28] T. Stanev et al., astro-ph/0003484.
- [29] C. Caso et al. (Particle Data Group), Eur. Phys. J. C3 (1998) 172.